Original Article

Application of high-frequency ultrasound in the early detection of pressure injury and evaluation of decompression treatment

Rongchen Wang, Xinyi Tang, Li Qiu, Liyun Wang

Department of Medical Ultrasound, West China Hospital, Sichuan University, Chengdu, China

Contributions: (I) Conception and design: L Wang, L Qiu, R Wang; (II) Administrative support: L Wang, L Qiu; (III) Provision of study materials or patients: L Wang, R Wang; (IV) Collection and assembly of data: L Qiu, R Wang; (V) Data analysis and interpretation: All authors; (VI) Manuscript writing: All authors; (VII) Final approval of manuscript: All authors.

Correspondence to: Liyun Wang, MD, PhD. Department of Medical Ultrasound, West China Hospital, Sichuan University, No. 37 Guoxue Alley, Chengdu 610041, China. Email: liyunwang1992@qq.com.

Background: Pressure injury (PI) is an ischemic necrosis caused by long-term pressure on the local skin, which is common in the sacrococcygeal region of long-term bedridden patients. The main treatment for PI is decompression. The Braden scale is the primary clinical evaluation tool for PI, but it cannot quantitatively evaluate PI. High-frequency ultrasound (HFUS) can be used for the real-time quantitative evaluation of PI. This study used HFUS to qualitatively and quantitatively assess the soft tissues of the sacrococcygeal region in different risk PI groups to investigate any differences in HFUS manifestations and evaluate the efficacy of decompression treatment in stage 1 PI patients.

Methods: A total of 70 patients were recruited from the Intensive Care Unit at West China Hospital, Sichuan University, of whom, 28 were allocated to the case group (a moderate or higher risk for PI, and a Braden score of 15–17) and 42 were allocated to the control group (a very mild risk for PI, and a Braden score ≥18). HFUS was used to measure tissue thickness and ultrasonographic characteristics, as well as blood flow signals at 10 target sites along the transverse plane from the sacral protrusion to the top. Differences between groups were compared, and diagnostic efficacy was evaluated by a receiver operating characteristic (ROC) curve analysis, and the area under the curve (AUC) was calculated. A subgroup of 12 extremely high-risk patients receiving decompression treatment was also examined. The HFUS parameters were compared before and after treatment to evaluate efficacy.

Results: In the case group, ultrasonographic uneven echo, unclear boundaries between adipose/muscular layers and dermis/adipose layers, and discontinuous deep/superficial fascia were more common closer to sacral protrusions ($P<0.05$). The case group had thinner median and paraspinal fat layers at all 10 sites than the control group ($P<0.05$). Certain sites (3, 5–7, and 9–10) in the case group had thicker epidermis ($P<0.05$), while the muscle layer was thinner at sites 5–10 of the case group ($P<0.01$). The ROC curve analysis indicated that the median and paraspinal fat layers could be used to effectively classify medium–high-risk patients with optimal performance at sites 3–5. The blood flow signal characteristics and composition ratios differed significantly between the case and control groups at each analyzed site ($P<0.05$). No significant changes in the Braden scores were found following decompression therapy, but the thickness of the paraspinal fat layer at sites 3 and 4 and the thickness of the median spinal fat layer at site 4 increased significantly ($P<0.05$). Further, the paraspinal fat layer thickness differed significantly between the initial and sixth ultrasound assessments ($P<0.05$). Most participants experienced reduced blood flow at the targeted site after decompression treatment.

Conclusions: HFUS enables the quantitative and qualitative assessment of soft tissues in the sacrococcygeal region and could be a valuable tool for predicting PI risks and evaluating treatment effectiveness.

Keywords: Musculoskeletal ultrasound; pressure ulcer; sacrococcygeal region; Braden score; decompression treatment

Submitted Aug 26, 2024. Accepted for publication Jan 23, 2025. Published online Feb 26, 2025.
doi: 10.21037/qims-24-1612
View this article at: https://dx.doi.org/10.21037/qims-24-1612

Introduction

Pressure injury (PI), also known as pressure ulcer (1), is a localized tissue injury and necrosis resulting from persistent ischemia, hypoxia, and malnutrition of the local skin or deep soft tissue under prolonged pressure (2,3). PI often occurs in areas of bony prominences and thin adipose tissue that are prone to compression, such as the sacrococcygeal region, calcaneus, elbow, and occipital region. Its etiology encompasses vertical pressure, friction, shear force, general nutritional disorders, and reduced skin resistance (4). Patients with severe conditions are susceptible to sacrococcygeal PI due to limited autonomous activity, poor nutritional status, and prolonged bed rest (5,6).

According to the National Pressure Ulcer Advisory Panel (NPUAP), PI can be classified into six categories based on the degree of skin tissue loss and clinical manifestations: stages 1–4; unstageable PI; and deep tissue PI (7). Stage 1 represents early stage PI (8). Clinical interventions for PI primarily involve managing tissue load (pressure, friction, and shear forces), providing nutritional support, caring for ulcers, and managing bacterial infections (9-11). The standard care for PI depends on its classification. Patients with early stage PI should undergo treatments such as pressure relief and skin protection to prevent progression toward advanced stages. In the late stage, debridement and dressing decompression are important measures for managing PI (12). The early detection of existing risk factors associated with PI along with accurate assessment and clinical intervention hold significant importance in improving patient prognosis, and reducing their physical, mental, and economic burdens (12).

At present, the Braden scale recommended by the NPUAP is widely used as the primary clinical assessment tool for PI worldwide (13). This scale evaluates PI based on six indicators (i.e., sensation, moisture, mobility, nutritional status, friction, and shear force). Each indicator is assigned a score ranging from 1 to 4 points (with the exception of friction and shear force, which is assigned a score ranging from 1 to 3 points), resulting in a total score between 6 and 23 points. A lower score is indicative of a heightened risk for developing PI; scores of 18–23 points indicate a very mild risk; scores of 15–17 points indicate a mild risk; scores of 13–14 points indicate a moderate risk; scores of 10–12 points indicate a high risk; and scores of ≤9 points indicate an extreme risk (13). However, the subjective nature of the semi-quantitative Braden score restricts its capacity to accurately predict and assess the overall risk of PI in individuals, and it cannot offer insights into specific anatomical sites, lesion severity, the extent of tissue involvement, disease progression, or post-intervention changes. Therefore, more accurate quantitative methods tailored specifically to clinical PI assessment urgently need to be developed to address the limitations associated with traditional scoring tools (14,15).

Imaging modalities commonly used for the evaluation of PI include magnetic resonance imaging (MRI) and high-frequency ultrasound (HFUS). MRI has increased sensitivity in detecting soft tissue injuries; however, its cost and limited ability to facilitate continuous bedside assessments of critically ill patients with restricted mobility present certain constraints (16).

HFUS is a high-resolution imaging tool that can accurately visualize and measure the anatomical structure of each skin layer while also enabling the observation of blood flow in the target tissue using the power Doppler mode. HFUS has distinct advantages such as dynamic real-time imaging, the absence of radiation exposure, affordability, and feasibility at the bedside that render it indispensable compared to other imaging modalities.

Previous studies have identified abnormal HFUS signs of PI including indistinct demarcation between tissue layers, indistinct demarcation between tissue layers, hypoechoic lesions, discontinuity of deep fascia, and heterogeneous hypoechoic areas (17,18). However, currently, there is no standardized methodological framework for evaluating sites and ultrasound parameters of PI. Additionally, no relevant investigations have been conducted examining ultrasound alterations in soft tissues before and after decompression treatment.

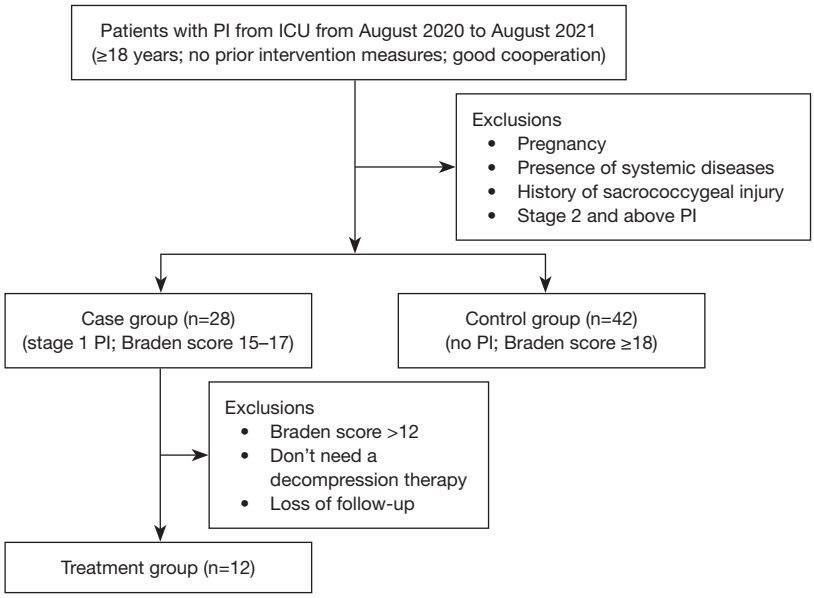

Figure 1 Diagram illustrating the process of case selection. ICU, intensive care unit; PI, pressure injury.

This study employed HFUS to evaluate the epidermis, dermis, adipose tissue, and muscle layers of the sacrococcygeal region in various risk groups for PI. Additionally, multiple HFUS follow-up assessments were conducted on patients undergoing decompression treatment. The study aimed to identify appropriate sites for HFUS evaluation of sacrococcygeal PI and investigate local soft tissue ultrasound manifestations in populations at risk for such injuries, as well as changes in ultrasound characteristics of tissues following decompression treatment. This study also aimed to provide quantitative and qualitative imaging indicators for clinically assessing the degree of risk associated with PI and evaluating treatment effectiveness. We present this article in accordance with the STROBE reporting checklist (available at https://qims.amegroups.com/article/view/10.21037/qims-24-1612/rc).

Methods

This cross-sectional study was conducted from August 2020 to August 2021 at West China Hospital, Sichuan University.

Research participants

Patients admitted to the Intensive Care Unit (ICU) at West China Hospital, Sichuan University between August 2020 and August 2021 were included in this study. Eligible patients were defined as those who had not yet developed a PI or were only at stage 1. Patients were excluded from the study if they had: (I) a history of diseases or injuries affecting soft tissues of the sacrococcygeal region; (II) previously received intervention measures such as debridement and dressing decompression treatment; (III) stage 2 and above PI; and/or (IV) Braden scores ≤14 points. Ultimately, 70 patients were included in the study. The case group comprised 28 patients with stage 1 PI only, who were classified as having a mild risk based on a Braden score of 15–17 points. While the control group comprised the remaining 42 patients, who were classified as having a very mild risk based on a Braden score ≥18 points, and who had no PI in the sacrococcygeal region. The patients in the case group were further allocated to the treatment group if they met the clinical criteria for decompression treatment (see *Figure 1*). Patients in the treatment group underwent Braden scale assessment and HFUS evaluations every three days following the initial assessment, with a minimum of two follow-up evaluations conducted, and up to five total evaluations performed.

Data collection and clinical assessment

Patients' demographic information, including gender, age, and body mass index (BMI), was collected for analysis. The Braden score was assessed by two experienced ICU nurses

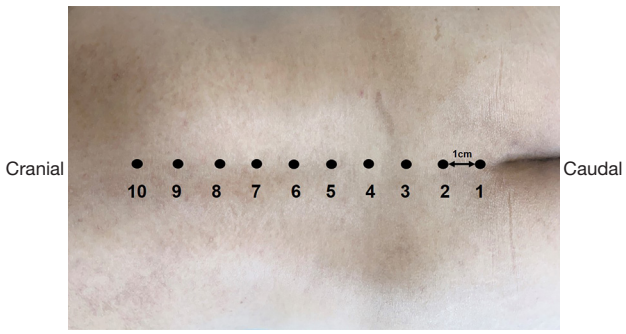

Figure 2 Diagram illustrating sites 1–10 in the HFUS examination of the sacrococcygeal region of patient. HFUS, high-frequency ultrasound.

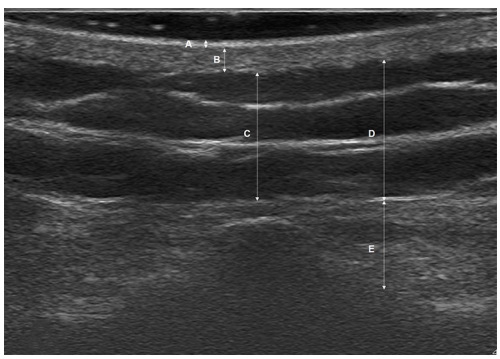

Figure 3 Ultrasonographic manifestations and thickness measurement of each skin layer. (A) Epidermis. (B) Dermis. (C) Median spinal fat layer. (D) Paraspinal fat layer. (E) Paraspinal muscle layer.

based on six indicators (i.e., sensation, moisture, mobility, nutritional status, friction and shear force). Each indicator was assigned a score ranging from 1 to 4 points (with the exception of friction and shear force, which were assigned a score ranging from1 to 3 points), resulting in a total score of 6–23 points.

HFUS examination

Ultrasound images were acquired using a Philips (CX50, Bothell, Washington, USA) color ultrasound diagnostic system equipped with a 5–12-MHz high-frequency linear array probe. The power Doppler settings were adjusted to optimize color gain just prior to the onset of color artifact. All patients underwent HFUS examination of the sacrococcygeal region conducted by a sonographer with over 5 years of experience (R.W.), and the acquired images were then collectively evaluated by a sonographer with more than 20 years of experience (L.Q.) and a sonographer with more than 10 years of experience (L.W.). A consistency check was also conducted.

The patient was placed in the left lateral decubitus position, with the body positioned perpendicular to the bed surface to expose the sacrococcygeal region. Initially, the examiner palpated the sacrococcygeal region starting from the sacral protrusion and then marked points at 1-cm intervals along the spine from the bottom to the top for a total of 10 sites (*Figure 2*). Subsequently, transverse scanning was performed at each site to obtain gray-scale ultrasound images of soft tissues. Measurements were obtained three times and averaged to determine the thickness of the epidermis, dermis, and fat layer on the median of the spine, as well as the fat and muscle layer on the paraspinal line (1.25 cm to the right of the spinal midline) (*Figure 3*). If the boundary of an anatomical level could not be visualized or quantified in an ultrasound image, it was recorded as 0. The blood flow in the soft tissue was observed using the power Doppler mode, and graded according to the Adler method as follows: Grade 0, no blood flow; Grade 1, a small amount of blood flow, characterized by 1–2 punctate or thin short rod vessels; Grade 2, moderate blood flow, indicated by 3 to 4 spots or one long blood vessel; and Grade 3, excessive blood flow, represented by more than 5 puncta or 2 longer vessels (19) (*Figure 4*).

Statistical analysis

The data were analyzed using SPSS 26.0 software (IBM Corp., Chicago, IL, USA, 2020). The counting data are expressed as the frequency and rate, and the differences between groups were compared using the x^2 test. The measurement data that did not conform to a normal distribution and showed homogeneity of variance are presented as the median (interquartile range) [i.e., the median (P25%, P75%)], and were compared between two groups using the Mann-Whitney *U* test. The Friedman test was used to compare differences between multiple groups of samples. Further pairwise comparisons were made using the test level α' (corrected by the Bonferroni method: α' = α/N, α is 0.05, where N represents the number of pairwise comparisons). The receiver operating characteristic (ROC) curve was used to evaluate diagnostic efficacy. In the ROC curve analysis, the results of multiple sites were first used as covariables by logistic regression to evaluate the risk of

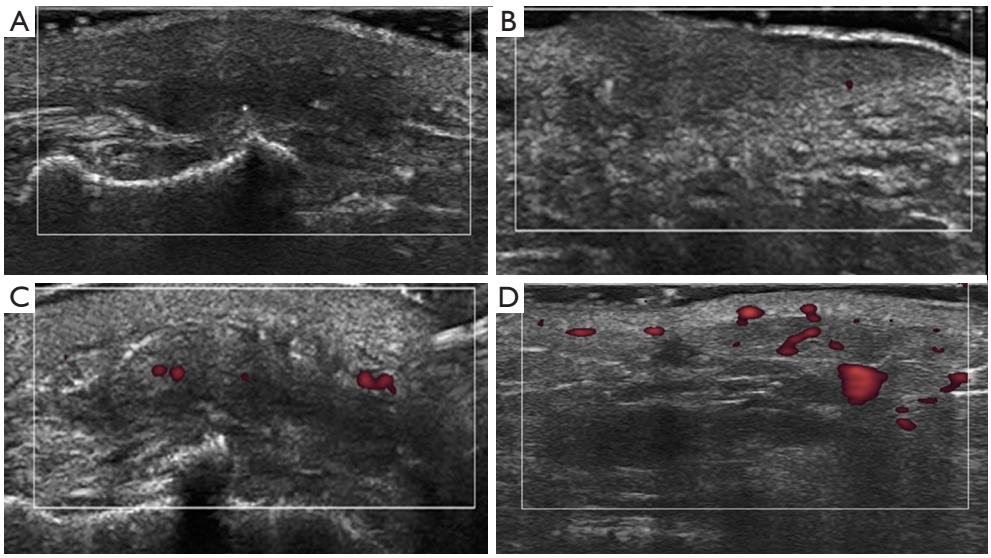

Figure 4 Diagram illustrating Adler grading of internal blood flow in pressure injure lesions. (A-D) represent grades 0–3, respectively.

Table 1 Demographic characteristics and Braden score of the case and control groups

Characteristics	Case group (n=28)	Control group (n=42)	P value
Gender (male:female)	21:7	32:10	0.909
Age (years)	48.5 (29.5–54.0)	31.5 (29.7–35.0)	<0.001
BMI (kg/m^2)	22.8 (18.8–24.7)	22.5 (20.6–24.7)	0.697
Braden score	12.0 (12.0–13.0)	23.0 (23.0–23.0)	<0.001

Data are presented as median (interquartile range) or number. BMI, body mass index.

PI. The "input" method was used for regression, and the corresponding prediction probability was saved, and the ROC curve was drawn for the final probability prediction. A P value <0.05 indicated that the difference was statistically significant, and the test was two-tailed.

Ethical statement

The study was conducted in accordance with the Declaration of Helsinki (as revised in 2013). The study was approved by the Institutional Review Board of West China Hospital, Sichuan University [approval No. 2021(1509)], and informed consent was obtained from all participants.

Results

Patient characteristics

A total of 70 ICU patients were included in this study, of whom, 28 were allocated to the case group and 42 were allocated to the control group. The age of the patients in the case group was significantly higher than that of the patients in the control group [48.5 (29.5–54.0) *vs.* 31.5 (29.7–35.0) years, P<0.001]; however, no significant differences were observed between the two groups in terms of the sex ratio or BMI (*Table 1*).

The value of HFUS features in the evaluation of PI

In the control group, only three patients demonstrated heterogeneous echo patterns in a few sites (≤2 sites). Although only patients with early PI were included in the case group, all patients exhibited at least one abnormal ultrasound sign, such as heterogeneous echogenicity of the skin, fat, and muscle layers, indistinct anatomical layer boundaries, and continuous or partial disruption of the fibrous septum within the superficial or deep fascia layer

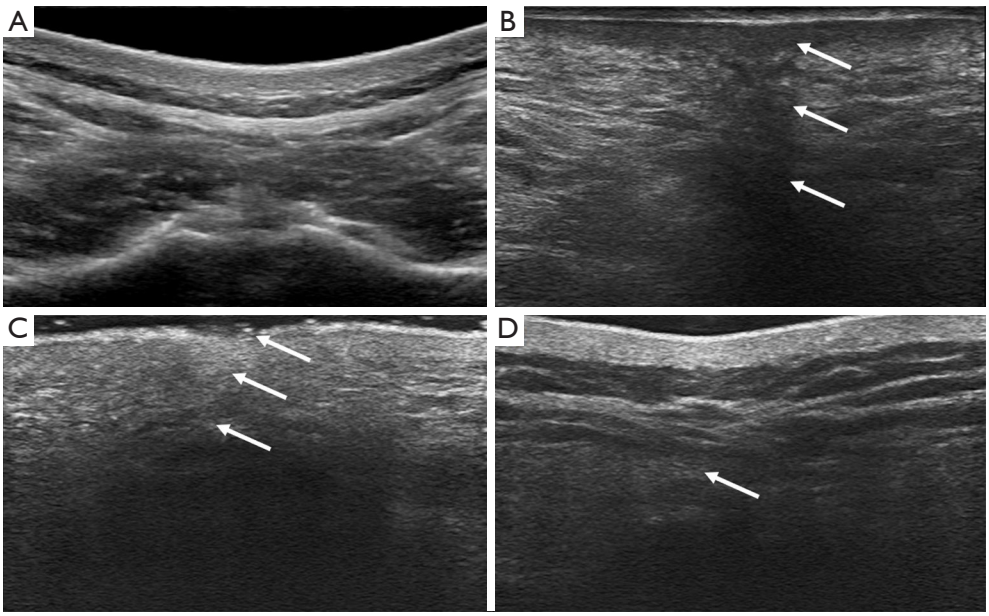

Figure 5 Normal and abnormal ultrasound images of the sacrococcygeal soft tissue. (A) Normal skin images. (B) Heterogeneous echoes observed in the skin, fat, and muscle layers (arrows). (C) Indistinct boundaries between the epidermis and dermis, as well as between the skin and adipose layer, and between the adipose and muscle layer (arrows). (D) Discontinuity of the deep fascia (arrows).

(*Figure 5*). In the case group, there were differences in the distribution of echo uniformity in both the skin and adipose layers at 10 sites, and there were differences in the boundary between the adipose layer and the muscle layer at 10 sites. In addition, the proportion of discontinuous fascial layer was higher in the case group than the control group, while the distribution of the proportion among various sites differed (*Tables 2-4*).

As *Figure 6* shows, as the sacral protrusion was approached, there was a corresponding rise in the prevalence of uneven ultrasound echoes in the skin, fat, and muscle layers, as well as discontinuities in both the deep and superficial fascia. In relation to the anatomical boundaries at each level, no significant association was found between the proportion of indistinct boundaries between the epidermis and dermis, and the sites; however, as the distance from the measurement point to the sacral protrusion increased, there was a decrease in the proportion of unclear boundaries between the dermis and adipose layer, as well as between the adipose and muscle layer. These findings are presented in *Table 3*. Our findings revealed that over 80% of patients with a moderate to very high risk of PI exhibited at least one of the aforementioned abnormal ultrasound signs at the origin of the sacrococcygeal process (site 1).

Comparison of soft tissue thickness at each site between the case and control groups

The patients in the case group had significantly higher epidermal thickness than those in the control group at sites 3, 5–7, and 9–10. Moreover, the patients in the case group had thinner median and paraspinal spine fat layers than those in the control group across all sites. Further, compared to the control group, a significant decrease in muscular layer thickness was observed in the case group at sites 5–10, but no differences were found at other sites. Additionally, minimal disparities in dermis thickness were only observed between the two groups at three sites (*Table 5*).

ROC curve analysis of soft tissue layer thickness at different sites

First, the overall thickness of the 10 sites was analyzed using logistic regression to examine the soft tissue thickness at different layers, and ROC curves were generated. The epidermal and paraspinal muscle thickness had area under the curve (AUC) values of 0.815 and 0.877 (*Figure 7A*,*7B*), respectively, indicating a moderate impact on risk classification. Conversely, the paraspinal fat layer and

Table 2 Echo uniformity of each layer at different sites in the case group

Site	Skin layer echo*		Adipose layer echo*		Muscular layer echo	
	Heterogeneous	Homogeneous	Heterogeneous	Homogeneous	Heterogeneous	Homogeneous
1	20 (71.4)	8 (28.6)	20 (71.4)	8 (28.6)	27 (96.4)	1 (3.6)
2	21 (75.0)	7 (25.0)	20 (71.4)	8 (28.6)	26 (92.9)	2 (7.1)
3	21 (75.0)	7 (25.0)	18 (64.3)	10 (35.7)	26 (92.9)	2 (7.1)
4	22 (78.6)	6 (21.4)	17 (60.7)	11 (39.3)	25 (89.3)	3 (10.7)
5	19 (67.9)	9 (32.1)	16 (57.1)	12 (42.9)	25 (89.3)	3 (10.7)
6	15 (53.6)	13 (46.4)	14 (50.0)	14 (50.0)	25 (89.3)	3 (10.7)
7	12 (42.9)	16 (57.1)	14 (50.0)	14 (50.0)	25 (89.3)	3 (10.7)
8	11 (39.3)	17 (60.7)	11 (39.3)	17 (60.7)	24 (85.7)	4 (14.3)
9	10 (35.7)	18 (64.3)	9 (32.1)	19 (67.9)	23 (82.1)	5 (17.9)
10	10 (35.7)	18 (64.3)	8 (28.6)	20 (71.4)	22 (78.6)	6 (21.4)

Data are presented as n (%). *, P<0.05.

Table 3 Clarity of the boundary of each layer at different sites in the case group

Site	Boundary between epidermis and dermis		Boundary between dermis and adipose layer*		Boundary between adipose and muscular layer*	
	Unclear	Clear	Unclear	Clear	Unclear	Clear
1	7 (25.0)	21 (75.0)	16 (57.1)	12 (42.9)	23 (82.1)	5 (17.9)
2	8 (28.6)	20 (71.4)	15 (53.6)	13 (46.4)	23 (82.1)	5 (17.9)
3	9 (32.1)	19 (67.9)	16 (57.1)	12 (42.9)	22 (78.6)	6 (21.4)
4	9 (32.1)	19 (67.9)	16 (57.1)	12 (42.9)	21 (75.0)	7 (25.0)
5	10 (35.7)	18 (64.3)	14 (50.0)	14 (50.0)	19 (67.9)	9 (32.1)
6	9 (32.1)	19 (67.9)	11 (39.3)	17 (60.7)	18 (64.3)	10 (35.7)
7	7 (25.0)	21 (75.0)	10 (35.7)	18 (64.3)	13 (46.4)	15 (53.6)
8	6 (21.4)	22 (78.6)	8 (28.6)	20 (71.4)	9 (32.1)	19 (67.9)
9	6 (21.4)	22 (78.6)	7 (25.0)	21 (75.0)	9 (32.1)	19 (67.9)
10	3 (10.7)	25 (89.3)	5 (17.9)	23 (82.1)	7 (25.0)	21 (75.0)

Data are presented as n (%). *, P<0.05.

median spine fat layer thickness had AUC values of 0.921 and 0.930 (*Figure 7C*,*7D*), respectively, in distinguishing between a moderate or higher risk, and very mild risk of PI, highlighting their significant influence on risk classification.

Further, individual ROC curve analyses were conducted of the soft tissue layer thickness of each site, and heat maps visually displaying the corresponding AUC values were generated (*Figure 8*); lighter colors indicated closer proximity to an AUC value of 1, representing stronger classification efficacy; while darker colors indicated closer proximity to an AUC value of 0.5, indicating weaker classification efficacy. In terms of efficacy in classifying the PI risks of individual layers at each site, the performance of epidermal thickness and paraspinal muscle layer thickness was found to be suboptimal (AUC =0.563–0.713). Conversely, paraspinal (AUC =0.674–0.900) and median spine fat layer thickness (AUC =0.732–0.929) exhibited superior classification efficacy with higher overall AUC

values, particularly at sites 3–5. The classification efficacy of paraspinal muscle layer thickness on PI risk varied across different sites, and an enhanced effect was observed as the distance from the sacral protrusion increased (AUC =0.468–0.829). Overall, fat layer thickness played a crucial role in classifying ICU patients' risk of PI development, particularly when considering the paraspinal and median spine fat layers near sites 3–5.

The value of power Doppler ultrasound in the evaluation of PI

In the control group, the soft tissue of all 10 sites had blood flow signals between grades 0 and 1. However, in the case group, different proportions and grades of blood flow signals were detected at all 10 sites, and statistically significant differences in the distribution of blood flow grades were observed between the two groups. Further, the patients in the case group had a higher proportion of detectable power Doppler blood flow signals (including an Adler grade ≥2) within a distance of 6 cm above the sacral protrusion, and the ultrasonically detectable blood flow signals decreased as the distance from the sacral protrusion increased (*Table 6*).

Table 4 Continuity of the deep and superficial fascia at different sites in the case group

Site	Deep fascia*		Superficial fascia*	
	Discontinuous	Continuous	Discontinuous	Continuous
1	25 (89.3)	3 (10.7)	16 (57.1)	12 (42.9)
2	22 (78.6)	6 (21.4)	16 (57.1)	12 (42.9)
3	20 (71.4)	8 (28.6)	17 (60.7)	11 (39.3)
4	17 (60.7)	11 (39.3)	15 (53.6)	13 (46.4)
5	15 (53.6)	13 (46.4)	13 (46.4)	15 (53.6)
6	15 (53.6)	13 (46.4)	12 (42.9)	16 (57.1)
7	13 (46.4)	15 (53.6)	12 (42.9)	16 (57.1)
8	11 (39.3)	17 (60.7)	9 (32.1)	19 (67.9)
9	12 (42.9)	16 (57.1)	8 (28.6)	20 (71.4)
10	9 (32.1)	19 (67.9)	5 (17.9)	23 (82.1)

Data are presented as n (%). *, P<0.05.

HFUS assessment of treatment effectiveness decompression therapy in PI

In this study, the case group initially comprised 16 patients who were clinically assessed as requiring dressing decompression treatment; however, within 3 days, 4 patients were transferred out of the ICU for various reasons. Consequently, the HFUS follow-up evaluation was conducted on a total of 12 subjects. Based on the aforementioned findings, the paraspinal and median spine fat layers at sites 3–5 were consistently assessed in all 12 patients during each ultrasound evaluation session. Simultaneously, the clinical Braden scale was completed on the same day as each ultrasound assessment. Assessments were performed every 3 days for a total of five times after treatment initiation.

No significant changes in the Braden scores were observed during the follow-up period. However, as *Table 7* shows, a significant increase in the paraspinal fat layer thickness at sites 3 and 4 was noted during the ultrasound evaluations. Further comparisons revealed a significant difference in the paraspinal fat layer thickness between the first and sixth ultrasound evaluations (prior to treatment: 7.92 and 5.02 mm for sites 3 and 4, respectively; after five treatments: 8.64 and 8.16 mm, respectively). Additionally, site 4 showed a

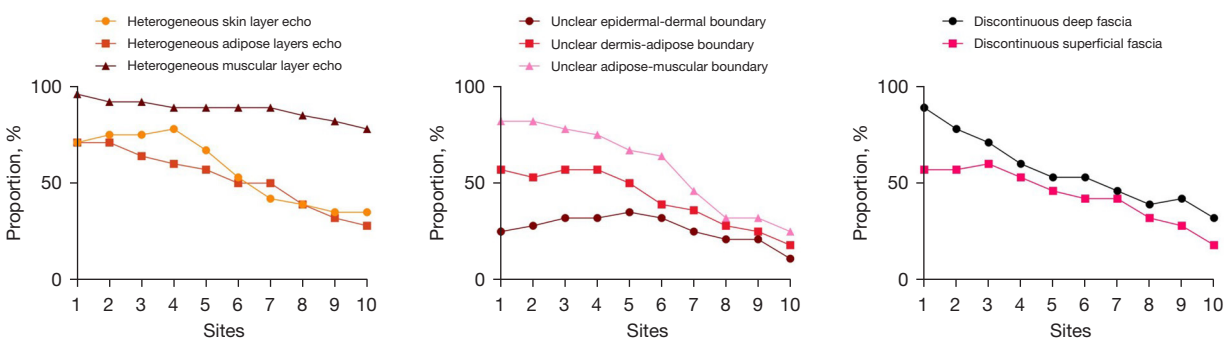

Figure 6 The proportion of abnormal ultrasound signs at sites 1–10 in the case group.

Table 5 Comparison of soft tissue thickness at sites 1–10 between the case and control groups

Site	Layer	Thickness (mm)		P value
		Case group (n=28)	Control group (n=42)	
1	Epidermis	0.50 (0.46–0.59)	0.45 (0.40–0.52)	0.083
	Dermis	2.85 (2.48–3.56)	3.44 (3.02–3.78)	0.020
	Median spinal fat layer	1.91 (0.00–4.19)	10.10 (5.87–15.53)	<0.001
	Paraspinal fat layer	2.93 (0.00–5.95)	11.70 (7.21–16.05)	<0.001
	Paraspinal muscle layer	12.95 (11.23–16.38)	13.55 (10.55–16.75)	0.815
2	Epidermis	0.50 (0.45–0.64)	0.45 (0.40–0.50)	0.061
	Dermis	3.00 (2.45–3.80)	3.35 (3.09–3.81)	0.100
	Median spinal fat layer	1.55 (0.00–4.32)	8.23 (6.60–13.33)	<0.001
	Paraspinal fat layer	3.66 (1.86–6.47)	12.20 (6.10–15.90)	<0.001
	Paraspinal muscle layer	14.20 (9.40–17.63)	13.40 (10.10–16.65)	0.653
3	Epidermis	0.50 (0.43–0.60)	0.45 (0.40–0.50)	0.036
	Dermis	3.15 (2.47–3.71)	3.27 (2.82–3.63)	0.294
	Median spinal fat layer	1.88 (0.00–4.03)	9.53 (5.80–13.80)	<0.001
	Paraspinal fat layer	3.47 (0.24–6.36)	13.40 (8.34–15.80)	<0.001
	Paraspinal muscle layer	11.30 (10.05–14.25)	12.30 (8.79–16.53)	0.439
4	Epidermis	0.49 (0.39–0.54)	0.45 (0.40–0.50)	0.371
	Dermis	2.83 (2.46–3.40)	3.18 (2.86–3.81)	0.016
	Median spinal fat layer	3.22 (0.00–4.38)	11.50 (6.37–14.20)	<0.001
	Paraspinal fat layer	4.06 (1.93–5.78)	12.90 (8.74–15.13)	<0.001
	Paraspinal muscle layer	11.60 (9.94–14.70)	13.40 (10.27–17.08)	0.314
5	Epidermis	0.50 (0.42–0.62)	0.43 (0.40–0.50)	0.012
	Dermis	2.85 (2.49–3.49)	3.15 (2.86–3.44)	0.092
	Median spinal fat layer	4.06 (1.31–5.80)	11.55 (7.47–13.90)	<0.001
	Paraspinal fat layer	4.90 (1.48–7.55)	12.25 (9.53–15.20)	<0.001
	Paraspinal muscle layer	11.60 (9.67–13.00)	15.60 (12.60–19.48)	<0.001
6	Epidermis	0.47 (0.44–0.51)	0.41 (0.39–0.50)	0.018
	Dermis	2.88 (2.34–3.48)	3.01 (2.78–3.44)	0.320
	Median spinal fat layer	4.68 (0.69–6.15)	10.90 (7.69–14.68)	<0.001
	Paraspinal fat layer	4.50 (3.04–6.78)	11.90 (8.70–15.20)	<0.001
	Paraspinal muscle layer	11.35 (9.84–14.00)	17.60 (14.08–20.38)	<0.001
7	Epidermis	0.50 (0.42–0.65)	0.45 (0.40–0.49)	0.025
	Dermis	2.73 (2.40–3.40)	2.91 (2.65–3.36)	0.267
	Median spinal fat layer	4.54 (3.06–7.28)	11.25 (8.66–14.98)	<0.001
	Paraspinal fat layer	4.73 (2.97–8.79)	10.65 (8.02–13.25)	<0.001
	Paraspinal muscle layer	11.70 (10.33–15.63)	20.80 (16.08–24.00)	<0.001

Table 5 (*continued*)

Table 5 (*continued*)

Site	Layer	Thickness (mm)		P value
		Case group (n=28)	Control group (n=42)	
8	Epidermis	0.47 (0.36–0.55)	0.40 (0.40–0.48)	0.227
	Dermis	2.63 (2.33–3.38)	2.98 (2.79–3.39)	0.058
	Median spinal fat layer	5.79 (3.18–7.30)	11.75 (8.46–14.55)	<0.001
	Paraspinal fat layer	5.20 (2.61–8.03)	9.53 (6.97–13.10)	<0.001
	Paraspinal muscle layer	13.45 (11.35–17.40)	23.55 (15.95–26.70)	<0.001
9	Epidermis	0.47 (0.40–0.63)	0.40 (0.40–0.48)	0.049
	Dermis	2.77 (2.40–3.34)	3.00 (2.56–3.35)	0.356
	Median spinal fat layer	6.61 (3.67–11.10)	12.30 (9.40–16.63)	<0.001
	Paraspinal fat layer	5.98 (3.17–8.93)	9.13 (5.51–11.23)	0.014
	Paraspinal muscle layer	15.75 (9.30–21.10)	26.10 (20.40–29.23)	<0.001
10	Epidermis	0.49 (0.45–0.62)	0.40 (0.40–0.46)	0.002
	Dermis	2.59 (2.32–3.01)	2.90 (2.58–3.22)	0.022
	Median spinal fat layer	7.81 (3.41–11.53)	11.60 (9.04–15.70)	0.001
	Paraspinal fat layer	5.30 (3.28–7.92)	7.34 (5.48–12.33)	0.006
	Paraspinal muscle layer	19.95 (11.98–24.35)	27.25 (20.18–30.28)	<0.001

Data are presented as median (interquartile range).

significant change in the median spine fat layer thickness (4.52–5.82 mm). As we found in a previous study that there was a higher proportion of detectable power Doppler flow signals within 6 cm (sites 1–7) above the sacral protrusion, we continuously monitored the blood flow signals in the paravertebral soft tissues at these sites in the 12 patients, and we found a significant decrease in the blood flow grade at the target sites following the decompression treatment (*Figure 9*).

Discussion

In PI prevention and treatment research, the development of an accurate and reliable method for assessing PI holds great importance for clinical diagnosis, intervention, and treatment effectiveness evaluation. Our research showed that HFUS allows for both the quantitative and qualitative evaluation of soft tissues in the sacrococcygeal region, enabling the differentiation between varying risk levels of PI and the assessment of the efficacy of decompression treatment for patients with PI.

In our study, the patients with a higher risk of PI as assessed by the Braden score were found to be older. This may be due to the fact that the Braden score incorporates factors such as mobility and nutritional status, both of which tend to be more decreased in older ICU patients than younger patients.

We observed that abnormal ultrasound findings in soft tissues may have some implications for the risk of PI. On ultrasound, the normal skin layer, subcutaneous fat layer, and muscle layer exhibit uniformity in terms of echogenicity. Specifically, the epidermis appears as a linear hyperechoic structure, the dermis displays ribbon-like medium echogenicity, the fat layer exhibits hypoechoic characteristics, and the muscle layer demonstrates iso-hypoechoic properties (20). Additionally, each anatomical structure has distinct boundaries while maintaining an intact continuity between the superficial fascia and deep fascia. In this study, although no PI lesions above stage 1 were observed in the sacrococcygeal region of the patients in the case group, various abnormal ultrasound signs were evident in the sacrococcygeal soft tissues, including echogenicity heterogeneity, indistinct boundaries between anatomical layers, and the complete or partial disruption of superficial fascia/deep fascia continuity. The uneven echogenicity at each level of ultrasound image primarily results from

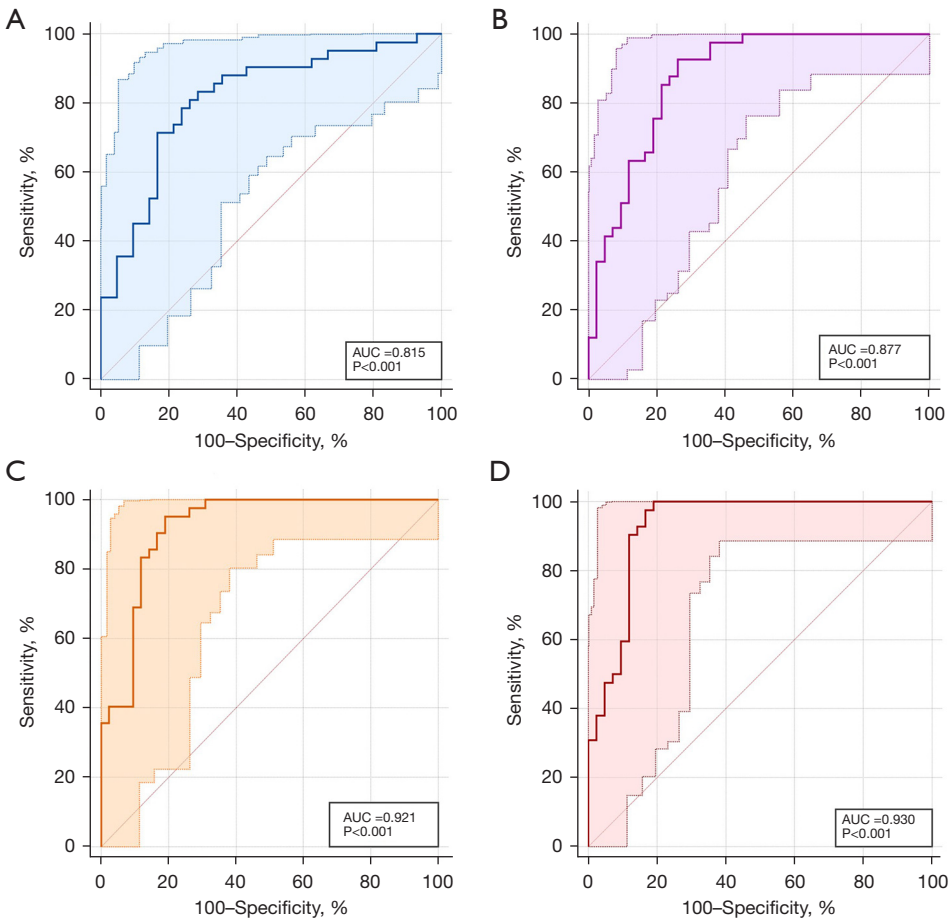

Figure 7 ROC curves of the overall soft tissue thickness of each layer for classification of different pressure injury risk groups. (A-D) correspond to the representation of the ROC curve of epidermal thickness, paraspinal muscle layer thickness, median spinal fat layer thickness, and paraspinal fat layer thickness, respectively. AUC, area under the curve; ROC, receiver operating characteristic.

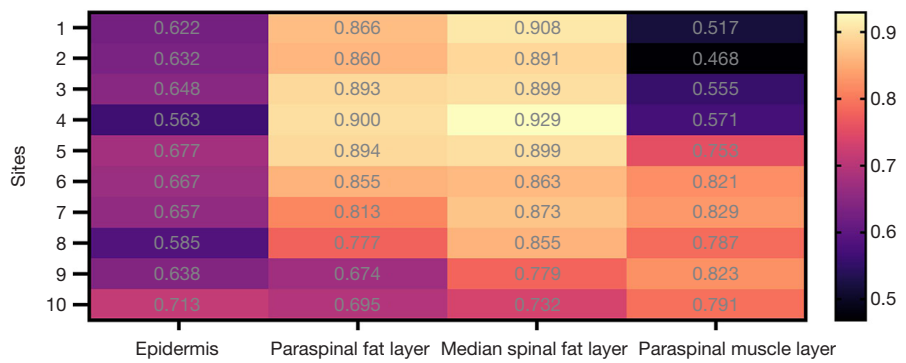

Figure 8 Heat map depicting the AUC values for soft tissue thickness at sites 1–10 across of pressure injury risk classification. AUC, area under the curve.

Table 6 Comparison of Adler blood flow grading for soft tissue at sites 1–10 between the case and control groups

Site	Group	Adler grade		P value
		0–1	≥2	
1	Case	23 (82.1)	5 (17.9)	0.008
	Control	42 (100.0)	0 (0.0)	
2	Case	23 (82.1)	5 (17.9)	0.008
	Control	42 (100.0)	0 (0.0)	
3	Case	24 (85.7)	4 (14.3)	0.022
	Control	42 (100.0)	0 (0.0)	
4	Case	23 (82.1)	5 (17.9)	0.008
	Control	42 (100.0)	0 (0.0)	
5	Case	22 (78.6)	6 (21.4)	0.003
	Control	42 (100.0)	0 (0.0)	
6	Case	23 (82.1)	5 (17.9)	0.008
	Control	42 (100.0)	0 (0.0)	
7	Case	23 (82.1)	5 (17.9)	0.008
	Control	42 (100.0)	0 (0.0)	
8	Case	26 (92.9)	2 (7.1)	0.157
	Control	42 (100.0)	0 (0.0)	
9	Case	25 (89.3)	3 (10.7)	0.060
	Control	42 (100.0)	0 (0.0)	
10	Case	27 (96.4)	1 (3.6)	0.400
	Control	42 (100.0)	0 (0.0)	

Data are presented as n (%).

localized edema, necrosis, and liquefaction caused by tissue ischemia and hypoxia along with subsequent ischemia-reperfusion injury during early stage PI (17). The local tissue destruction and inflammatory infiltration result in a reduction of regional contrast between the anatomical levels of each tissue on the ultrasound image, leading to indistinct boundaries. The presence of fascial discontinuity reflects local injury or even rupture, indicating the existence of deep tissue damage (17). Previous research has established that discontinuity in the fascial layer and irregular echo or hypoechoic areas at various soft tissue levels on ultrasound images are indicative of an elevated risk of PI progression, which aligns with our findings (18). Further, this study also observed variations in ultrasound signs across different sites, including a higher incidence of abnormal ultrasound signs observed closer to the sacral protrusion. This observation may be attributed to increased pressure and friction exerted on the sacral protrusion and its surrounding soft tissue, leading to heightened tissue damage (15).

Further, on HFUS, the epidermis of early stage PI patients was found to be thickened, while the subcutaneous fat layer and muscle layer appeared to be thinner. Ultrasound can identify changes in the subcutaneous layer of the low-risk group at an early stage. The pressure sores in the early stage are mainly characterized by thickening and edema, and the ultrasonic manifestation is epidermal layer thickening.

In terms of skin type, on the Braden scale, skin edema is related to the thickness of the skin layer, and BMI is related to the thickness of the subcutaneous fat. The observed

Table 7 Thickness measured by ultrasound of the paraspinal the median spine fat layer at sites 3–5 following decompression treatment

Thickness (mm)	Site	Frequency of ultrasound follow-up visits						P value
		1* (n=16)	2 (n=12)	3 (n=12)	4 (n=12)	5 (n=12)	6 (n=12)	
Paraspinal fat layer	3	7.92 (4.12–13.10)[a]	9.47 (4.13–15.18)[a]	6.35 (2.87–13.57)[a]	7.29 (4.37–15.19)[a]	8.30 (1.61–20.54)[a]	8.64 (4.24–22.72)[b]	0.019
	4	5.02 (4.23–10.44)[a]	7.54 (4.69–13.88)[a]	5.32 (2.99–12.51)[a]	5.29 (3.44–13.33)[a]	6.02 (1.59–16.12)[a]	8.16 (2.76–18.73)[b]	0.017
	5	5.03 (3.84–5.52)	5.02 (3.89–9.82)	4.84 (2.90–8.37)	4.94 (2.09–7.98)	5.02 (0.00–5.02)	7.29 (1.30–15.49)	0.185
Median spinal fat layer	3	5.36 (2.76–10.80)	5.99 (2.96–11.23)	5.82 (3.63–11.04)	6.13 (4.47–11.85)	6.67 (2.45–11.97)	7.02 (4.68–11.83)	0.078
	4	4.52 (2.68–5.33)[a]	4.86 (3.69–6.29)[a]	4.66 (2.74–6.18)[a]	4.47 (1.89–6.19)[a]	4.59 (0.00–7.72)[a]	5.82 (1.64–7.77)[a]	0.016
	5	4.10 (3.13–6.96)	4.19 (2.78–5.30)	4.37 (3.87–5.60)	4.30 (3.34–5.78)	4.26 (0.00–6.43)	4.68 (1.84–7.01)	0.088

*, the first ultrasound assessment was performed before the decompression treatment. [a, b], each letter indicates that in pairwise comparisons of different ultrasound assessments of fat layer thickness at the corresponding site, these thickness values do not differ significantly from each other at the 0.05 level.

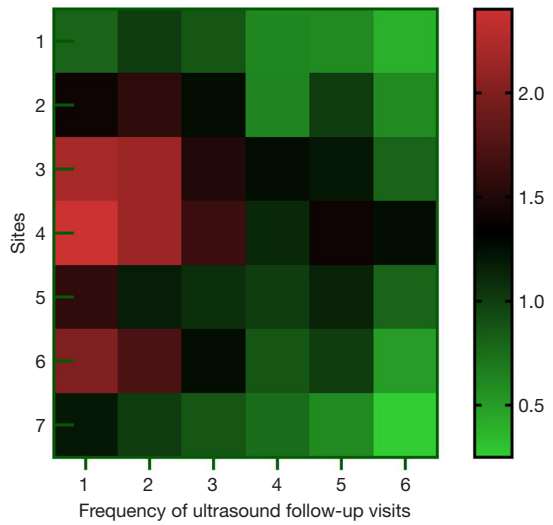

Figure 9 Heat map illustrating changes in average blood flow grading of soft tissue after decompression treatment at sites 1–7 in the treatment group. Each small square represents the average blood flow grading of 12 patients in the treatment group at each site.

thickening of the epidermal layer in the case group may be attributed to prolonged contact and repetitive friction between the sacrococcygeal skin and the bed surface during extended periods of bed rest, leading to damage and the subsequent thickening of the corneum. However, the Braden scale also includes five aspects (i.e., as sensation, moisture, mobility, friction and shear force). We mainly compared the thickness in the low-risk patients and normal individuals. Notably, changes in the skin and subcutaneous layer thickness cannot be evaluated solely based on the Braden score.

In relation to the subcutaneous fat layer, a previous study reported a significant correlation between its thickness and BMI, but not age (21). Our study found a difference in age but not in BMI between the case and control groups, indicating that variations in fat layer thickness are not solely due to demographic differences. Additionally, PI was not affected by BMI. The thinning of the subcutaneous fat layer may also be associated with inactivity, impaired sensory perception, and malnutrition, and may lead to an increased risk of PI after thinning. It is more likely that patients have different risks of PI because of varying levels of fat layer thickness (22). Fat frequently serves as a natural buffer, facilitating the more uniform distribution of stress (23). The presence of a thicker subcutaneous fat layer is specifically advantageous in protecting local compressed tissue and reducing the likelihood of PI occurrence, as demonstrated by characteristics observed among individuals at higher risk with relatively thinner fat layers.

In relation to the disparity in muscle layer thickness, the paraspinal muscle layer in the case group may experience more pronounced local compression, resulting in its reduced thickness compared to that in the control group, which aligns with the findings reported by Kitamura *et al.* (17). Additionally, it is important to note that as individuals progress beyond middle age, there is a natural decline in overall muscle mass (24,25), and thus the advanced age of the patients in the case group might also have contributed to their thinner muscle layer.

The thinning of muscle layers may also be associated with inactivity, impaired sensory perception, and malnutrition, and thinning may lead to an increased risk of PI. When the fat layer and the muscle layer have a tendency toward thinness, the patient may be at an increased risk of PI. Additionally, there was no significant difference in the dermal thickness observed between the two groups in this study. This finding may be attributed to the inclusion of early stage PI patients who did not present with macroscopic lesions during the evaluation, as well as the progression of PIs from the deep to superficial layers (4). Based on these findings, it may be challenging to observe early stage discernible dermal lesions using HFUS, which may create potential difficulties for accurate detection.

The results of the analysis on the difference in thickness for each anatomical layer between the two groups were further validated by the ROC curve analysis. Specifically, it was found that the thickness value of the paraspinal and median spine fat layer had high diagnostic efficacy in identifying a medium–high-risk of PI, and an AUC exceeding 0.85. Limited research has been conducted on the diagnostic efficacy of adipose layer thickness in PI; however, it has been suggested that the peripheral adipose layer may serve as a protective factor for PI. Compher *et al.* proposed that an increased fat layer may act as a protective mechanism by redistributing high interfacial pressure (26). Further, a previous study recommended fat grafting for pressure ulcers, which has shown effectiveness in preventing the development of these ulcers during the early stages (22).

Additionally, alongside gray-scale ultrasound findings, variations in blood flow signals were observed among the different PI risk groups, such that a higher proportion of blood flow signals were detected at each site in the case group compared to the control group. Histologically, PI can induce local inflammation characterized by inflammatory

edema and vascular dilatation in the skin layer and subcutaneous fat layer (27,28), leading to increased blood flow signals on ultrasound images. Therefore, the detection of abundant blood flow signals may indicate an abnormal inflammatory response in local soft tissues, suggesting an elevated risk of PI. The proportion of detectable blood flow signals within 6 cm above the sacrococcygeal protrusion was notably high, decreasing gradually as the distance from the sacrococcygeal protrusion increased, which exhibited a similar trend with the distribution observed for abnormal ultrasound signs. PI tends to occur at the bony prominences placed under the greatest pressure. If the patient is bedridden, these sites tend to be the sacrum, coccyx, trochanter, and calcaneus (4). All the patients enrolled in this study were ICU patients confined to bed rest; thus, there was a more pronounced presence of abnormalities closer to the sacrococcygeal region.

During the follow-up period, it was observed that following decompression treatment, there was no significant decrease in the Braden score of the patients. However, the ultrasound examinations revealed the thickening of the median and paraspinal fat layer to varying degrees, indicating the alleviation of local soft tissue pressure and an improvement in condition post-intervention. Additionally, the heat map analysis revealed a reduction in the blood flow signal in the soft tissue of the patients after decompression treatment, suggesting a decrease in the inflammatory response, and providing some evidence of the efficacy of decompression treatment.

This study had several limitations. First, due to early clinical interventions, only early stage PI patients were included in the study. Moreover, the use of relevant clinical interventions hindered the observation of natural disease progression and the outcomes associated with PIs, thereby restricting a comprehensive interpretation of the relationship between the ultrasound findings and disease prognosis. Second, the follow-up period was relatively short in this study, restricting our observation of ultrasound changes. Additionally, other imaging modalities or evaluation measures were not introduced as references or comparisons. Further, in ICU patients, rapid disease progression and the short duration of ICU treatment led to a smaller sample size with fewer patients available for follow-up and a shorter follow-up period. Further research should be conducted to determine the efficacy of HFUS in diagnosing PI, thereby establishing its validity and reliability for future clinical applications.

Conclusions

HFUS enables both the qualitative and quantitative assessment of soft tissue in the sacrococcygeal region, elucidating disparities in ultrasound measurements and sonographic characteristics among patients with mild PI. Moreover, it exhibits sensitivity in detecting alterations in local soft tissue morphology and blood flow signals after decompression treatment. Thus, it could serve as a potential tool for predicting PI risk and evaluating treatment efficacy in future clinical settings.

Acknowledgments

None.

Footnote

Reporting Checklist: The authors have completed the STROBE reporting checklist. Available at https://qims.amegroups.com/article/view/10.21037/qims-24-1612/rc

Funding: This work was financially sponsored by the National Natural Science Foundation of China (No. 82102065), and the Sichuan Science and Technology Program (No. 2024NSFSC1777).

Conflicts of Interest: All authors have completed the ICMJE uniform disclosure form (available at https://qims.amegroups.com/article/view/10.21037/qims-24-1612/coif). The authors have no conflicts of interest to declare.

Ethical Statement: The authors are accountable for all aspects of the work in ensuring that questions related to the accuracy or integrity of any part of the work are appropriately investigated and resolved. The study was conducted in accordance with the Declaration of Helsinki (as revised in 2013). The study was approved by the Institutional Review Board of West China Hospital, Sichuan University [approval No. 2021(1509)], and informed consent was obtained from all participants.

References

1. Sugathapala RDUP, Latimer S, Balasuriya A, Chaboyer W, Thalib L, Gillespie BM. Prevalence and incidence of pressure injuries among older people living in nursing homes: A systematic review and meta-analysis. Int J Nurs Stud 2023;148:104605.
2. Helvig EI, Nichols LW. Use of high-frequency ultrasound to detect heel pressure injury in elders. J Wound Ostomy Continence Nurs 2012;39:500-8.
3. Higashino T, Nakagami G, Kadono T, Ogawa Y, Iizaka S, Koyanagi H, Sasaki S, Haga N, Sanada H. Combination of thermographic and ultrasonographic assessments for early detection of deep tissue injury. Int Wound J 2014;11:509-16.
4. Headlam J, Illsley A. Pressure ulcers: an overview. Br J Hosp Med (Lond) 2020;81:1-9.
5. Sunn G. Spinal cord injury pressure ulcer treatment: an experience-based approach. Phys Med Rehabil Clin N Am 2014;25:671-80, ix.
6. Alshahrani B, Sim J, Middleton R. Nursing interventions for pressure injury prevention among critically ill patients: A systematic review. J Clin Nurs 2021;30:2151-68.
7. Edsberg LE, Black JM, Goldberg M, McNichol L, Moore L, Sieggreen M. Revised National Pressure Ulcer Advisory Panel Pressure Injury Staging System: Revised Pressure Injury Staging System. J Wound Ostomy Continence Nurs 2016;43:585-97.
8. Oliveira AL, Moore Z, O Connor T, Patton D. Accuracy of ultrasound, thermography and subepidermal moisture in predicting pressure ulcers: a systematic review. J Wound Care 2017;26:199-215.
9. McInnes E, Jammali-Blasi A, Bell-Syer SE, Dumville JC, Middleton V, Cullum N. Support surfaces for pressure ulcer prevention. Cochrane Database Syst Rev 2015;2015:CD001735.
10. Dinh A, Bouchand F, Davido B, Duran C, Denys P, Lortat-Jacob A, Rottman M, Salomon J, Bernard L. Management of established pressure ulcer infections in spinal cord injury patients. Med Mal Infect 2019;49:9-16.
11. Hill JE, Edney S, Hamer O, Williams A, Harris C. Interventions for the treatment and prevention of pressure ulcers. Br J Community Nurs 2022;27:S28-36.
12. Scafide KN, Narayan MC, Arundel L. Bedside Technologies to Enhance the Early Detection of Pressure Injuries: A Systematic Review. J Wound Ostomy Continence Nurs 2020;47:128-36.
13. Huang C, Ma Y, Wang C, Jiang M, Yuet Foon L, Lv L, Han L. Predictive validity of the braden scale for pressure injury risk assessment in adults: A systematic review and meta-analysis. Nurs Open 2021;8:2194-207.
14. Jansen RCS, Silva KBA, Moura MES. Braden Scale in pressure ulcer risk assessment. Rev Bras Enferm 2020;73:e20190413.
15. Lewicki LJ, Mion LC, Secic M. Sensitivity and specificity of the Braden Scale in the cardiac surgical population. J Wound Ostomy Continence Nurs 2000;27:36-41.
16. Doridam J, Macron A, Vergari C, Verney A, Rohan PY, Pillet H. Feasibility of sub-dermal soft tissue deformation assessment using B-mode ultrasound for pressure ulcer prevention. J Tissue Viability 2018;27:238-43.
17. Kitamura A, Yoshimura M, Nakagami G, Yabunaka K, Sanada H. Changes of tissue images visualised by ultrasonography in the process of pressure ulcer occurrence. J Wound Care 2019;28:S18-22.
18. Aoi N, Yoshimura K, Kadono T, Nakagami G, Iizuka S, Higashino T, Araki J, Koshima I, Sanada H. Ultrasound assessment of deep tissue injury in pressure ulcers: possible prediction of pressure ulcer progression. Plast Reconstr Surg 2009;124:540-50.
19. Adler DD, Carson PL, Rubin JM, Quinn-Reid D. Doppler ultrasound color flow imaging in the study of breast cancer: preliminary findings. Ultrasound Med Biol 1990;16:553-9.
20. Liu ZF, Chew CY, Honavar S, Maxwell A, Sylivris A, Sheridan A. Seeing beyond skin deep: High-resolution ultrasound in dermatology-A comprehensive review and future prospects. J Eur Acad Dermatol Venereol 2024;38:1305-13.
21. Hexsel D, Dal'Forno Dini T, Belem L, Tanure Correa I, Brandão A. Gluteal subcutaneous adipose tissue in women of different ages and body mass index observed by magnetic resonance imaging. J Cosmet Dermatol 2022;21:2169-75.
22. Vathulya M, Chattopadhyay D, Kandwal P, Nath UK, Kapoor A, Sinha M. Adipose Tissue in Peripheral Obesity as an Assessment Factor for Pressure Ulcers. Adv Wound Care (New Rochelle) 2023;12:513-28.
23. Nancy GA, Kalpana R, Nandhini S. A Study on Pressure Ulcer: Influencing Factors and Diagnostic Techniques. Int J Low Extrem Wounds 2022;21:254-63.

24. Kim WJ, Shin HM, Lee JS, Song DG, Lee JW, Chang SH, Park KY, Choy WS. Sarcopenia and Back Muscle Degeneration as Risk Factors for Degenerative Adult Spinal Deformity with Sagittal Imbalance and Degenerative Spinal Disease: A Comparative Study. World Neurosurg 2021;148:e547-55.
25. Pillen S, Arts IM, Zwarts MJ. Muscle ultrasound in neuromuscular disorders. Muscle Nerve 2008;37:679-93.
26. Compher C, Kinosian BP, Ratcliffe SJ, Baumgarten M. Obesity reduces the risk of pressure ulcers in elderly hospitalized patients. J Gerontol A Biol Sci Med Sci 2007;62:1310-2.
27. Gefen A, Gershon S. An Observational, Prospective Cohort Pilot Study to Compare the Use of Subepidermal Moisture Measurements Versus Ultrasound and Visual Skin Assessments for Early Detection of Pressure Injury. Ostomy Wound Manage 2018;64:12-27.
28. Yabunaka K, Iizaka S, Nakagami G, Aoi N, Kadono T, Koyanagi H, Uno M, Ohue M, Sanada S, Sanada H. Can ultrasonographic evaluation of subcutaneous fat predict pressure ulceration? J Wound Care 2009;18:192, 194, 196 passim.

Cite this article as: Wang R, Tang X, Qiu L, Wang L. Application of high-frequency ultrasound in the early detection of pressure injury and evaluation of decompression treatment. Quant Imaging Med Surg 2025;15(3):2280-2295. doi: 10.21037/qims-24-1612